

Design and Synthesis of Transition State Analogs for Induction of Hydride Transfer Catalytic Antibodies

Josef Schröer, Michel Sanner, Jean-Louis Reymond,^{*,†} and Richard A. Lerner*

Departments of Molecular Biology and Chemistry, The Scripps Research Institute,
10666 North Torrey Pines Road, La Jolla, California 92037

Received November 21, 1996[®]

Alcohol dehydrogenases and related aldehyde reductase enzymes catalyze the oxidation of alcohols to aldehydes and the simultaneous reduction of a nicotinamide derivative (NAD⁺ or NADP⁺) to the corresponding 1,4-dihydronicotinamide. Herein we report the design and synthesis of a stable transition state analog for this hydride transfer process. Compound **1** is a rigid [3.2.2] bicyclic structure containing 3-piperidone oxime as a mimic for 1,4-dihydronicotinamide. The piperidone is held in the boat conformation corresponding to the transition state by a three-atom lactam bridge between N(1) and C(4). The oxime function mimics the carboxamide group in nicotinamide. The lactam nitrogen serves as an attachment point for the alkyl group of the alcohol substrate, and the amide oxygen atom mimics its hydroxyl group. Compound **1** was prepared in 10 steps from *N*-benzylpiperidone, functionalized with substrate and cofactor recognition elements into transition state analogs **2** and **3** and conjugated to carrier proteins for immunization. These novel analogs open the way for the exploration of the dehydrogenase reaction using catalytic antibodies.

Introduction

Stable transition state analogs of chemical reactions play a central role in enzymology. These analogs are often tight binding inhibitors of enzymes, and structural analysis of their complexes with enzymes helps resolve the site and geometry of catalytic sites and leads to structural understanding of enzymatic reaction mechanisms.¹ Transition state analogs can also be used in an "active" manner to prepare catalytic antibodies.² This approach provides a practical route to novel protein catalysts and thereby allows one to test in practice theoretical models for enzymatic catalysis.

Alcohol dehydrogenases are extremely important enzymes which catalyze hydride transfer between position 4 of a 1,4-dihydronicotinamide of a cofactor NAD (nicotinamide adenine dinucleotide) or NADP (nicotinamide adenine dinucleotide phosphate) and the carbonyl group of an aldehyde or ketone (Scheme 1).³ The thermodynamic balance of the process in water normally favors alcohol and pyridinium cation but is brought near equilibrium within the active site of dehydrogenases.⁴ The origin of catalysis and the geometry of the transition state have been the object of intense scientific debate in recent years. This debate is all the more remarkable given the fact that NADH was the first enzymatic cofactor discovered nearly 100 years ago.⁵

One of the fundamental difficulties in designing a transition state analog for such a hydride transfer is the

Scheme 1. Hydride Transfer between 1,4-Dihydronicotinamide and an Aldehyde

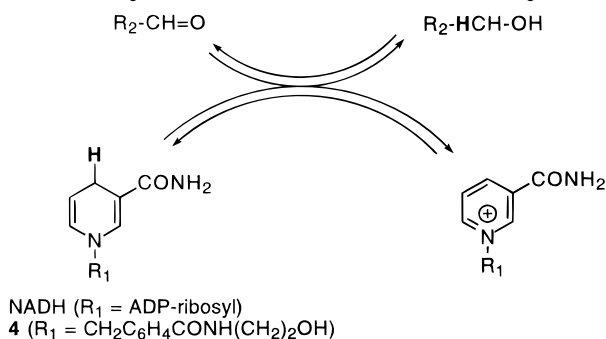
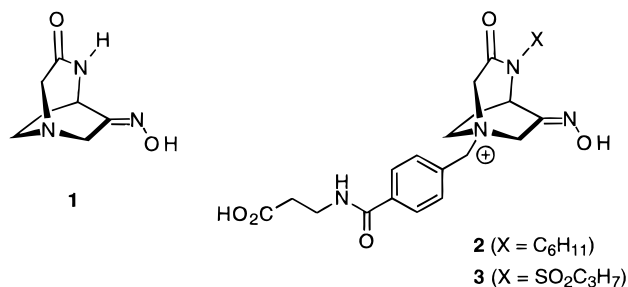


Chart 1



necessity to bring together a reactive cofactor and a substrate in a precise geometry within a hydrophobic environment. Herein we report the design and synthesis of a conformationally stable transition state analog **1** and its functionalization into haptens **2** and **3** for the preparation of catalytic antibodies (Chart 1). The model reaction is a hydride transfer between an *N*-benzyl-1,4-dihydronicotinamide **4** and an aldehyde (Scheme 1). This is an ideal reaction for study because the structure of the transition state has been defined by calculations.

Results and Discussion

Hundreds of inhibitors of alcohol dehydrogenases and of the related aldehyde reductases have been discovered in research programs directed at the inhibition of these enzymes for treatment of alcohol abuse and acute dia-

[†] Present address: Department of Chemistry & Biochemistry, University of Bern, 3012 Bern, Switzerland.

[®] Abstract published in *Advance ACS Abstracts*, April, 15, 1997.

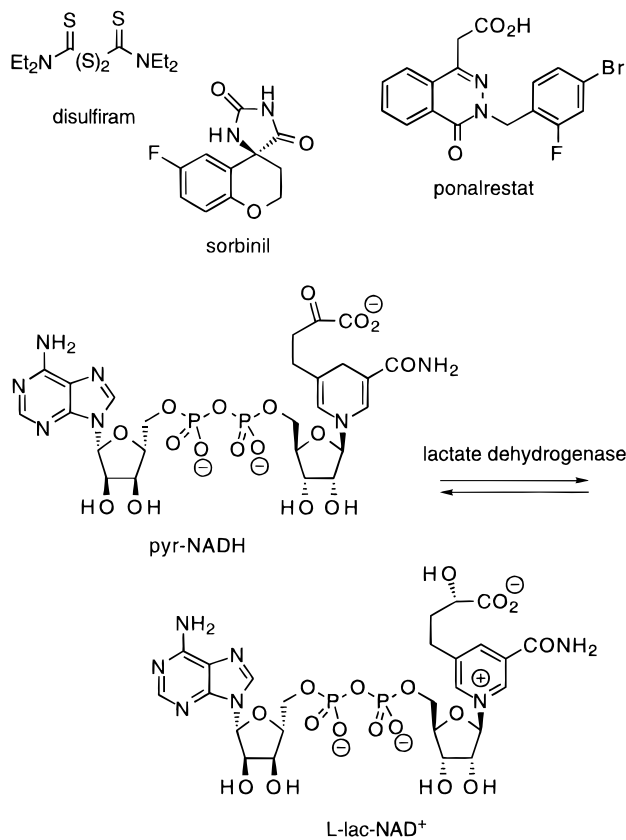
(1) For example: Haynes, M. R.; Stura, E. A.; Hilvert, D.; Wilson, I. A. *Science* **1994**, *263*, 646.

(2) (a) Schultz, P. G.; Lerner, R. A.; *Science* **1995**, *269*, 1835. (b) Lerner, R. A.; Benkovic, S. J.; Schultz, P. G. *Science* **1991**, *252*, 659.

(3) Rossman, M. G.; Liljas, A.; Brändén, C.-I.; Banaszak, L. J. Evolutionary and structural relationship among dehydrogenases. In *The Enzymes*; Academic Press, Inc.: New York, 1975; Vol. 11, p 61. (b) Oppenheimer, N. J.; Handlon, A. L. Mechanism of NAD-dependent enzymes. In *The Enzymes*; Academic Press, Inc.: New York, 1992; Vol. 20, p 453.

(4) Nambiar, K. P.; Stauffer, D. M.; Kolodziej, P. A.; Benner, S. A.; *J. Am. Chem. Soc.* **1983**, *105*, 5886.

(5) Harden, A.; Young, W. J. *Proc. R. Soc. B*, **1906**, *77*, 405 and 78, 369.

Chart 2. Examples of Alcohol Dehydrogenase Inhibitors

betes mellitus.⁶ Selected examples include disulfiram,⁷ sorbinil,⁸ and ponalrestat (Chart 2).⁹ Although many of these inhibitors are very potent, with inhibition constants in the nanomolar range, none are of the transition state analog type or even bear any structural relation to the cofactor and substrate involved in the enzymatic process. A better structural resemblance is found with pyr-NADH, a substrate-cofactor construct which undergoes conversion to L-lac-NAD⁺ under the action of lactate dehydrogenase, and competitively inhibits this enzyme with $K_i = 1.35 \times 10^{-7}$ M.¹⁰ However, despite being clearly related to the actual enzymatic reaction, this substrate construct is not formally a transition state analog, and its conformational flexibility makes it an unlikely candidate for use as a template for a catalytic site in immunization.

Geometry of the Transition State. With the aim of inducing catalytic antibodies by immunization, we sought to design an accurate and conformationally stable transition state analog for the alcohol dehydrogenase reaction. Crystal structures of alcohol dehydrogenases as ternary complexes with both NAD⁺ and a substrate are available from the protein database. Although these do not provide a precise picture of the transition state, the coordinates have been used as a starting point for

computations.¹¹ A detailed geometrical description of the transition state was obtained for the hydride transfer process between methanol and NAD⁺ within the active site of several dehydrogenases. The problem has also been treated independently in gas phase calculations of the hydride transfer from 1,4-dihydropyridine to formaldehyde,¹² to a methylene imminium cation¹³ or to formaldehyde hydrogen bonded to an imidazole,¹⁴ as well as for the symmetrical transfer between 1,4-dihydroneicotinamide and protonated nicotinamide.¹⁵ Despite widely varying starting points and substrates, these studies agree well as to the overall geometry of the process.

In the calculated transition state of the enzymatic reaction, the 1,4-dihydroneicotinamide in NAD is present in a puckered boat conformation with $\alpha_N \approx 5^\circ$ and $\alpha_C \approx 15^\circ$ (Scheme 2). These values are slightly smaller in calculations involving 1,4-dihydropyridine because puckering strongly depends on the presence of an alkyl substituent at the pyridine nitrogen. The boat conformation can be reached by deformation of the planar 1,4-dihydropyridine ring in the ground state at little energetic cost (≈ 1.8 kcal/mol), and experimental evidence from Raman spectroscopic studies with stereospecifically deuterated NADH suggest that this is indeed the case for this cofactor in the enzyme-bound state.¹⁶ According to the calculation by Bruice et al.,¹¹ this boat conformation selectively lowers the transition state energy by as much as 6 kcal/mol, which makes it a key feature to be taken into account for transition state mimicry.

All the different calculation sources position the substrate carbonyl group approximately 3 Å above the dihydropyridine ring at the transition state. The results of Houk for dihydropyridine^{13,15} are representative: the breaking C(4)-H bond is elongated to approximately 1.21 Å, and the hydride attacks the carbonyl of the substrate at an angle of approximately 107° with a bond length of 1.46 Å, the C(4)-H-C angle being 158°. In these calculations the substrate C=N bond is placed in a symmetrical *syn* orientation above the pyridine ring. In the calculations for dogfish lactate dehydrogenase,¹¹ the orientation of the carbonyl is determined by a strong hydrogen-bonding interaction with a histidine residue on the enzyme. These calculations suggest that general acid-base catalysis by this residue plays a key role in enabling the hydride transfer to take place, and probably governs the orientation of the carbonyl group at the transition state.

Ring puckering and positioning of the carbonyl define the position that substrate and cofactor should adopt in space relative to one another. Together with the requirement for general acid-base catalysis for activation of the carbonyl substrate, these parameters are the most important to incorporate in a transition state mimic.

Further important parameters include the torsion angle of the carboxamide substituent at position 3 of the dihydropyridine, χ_{am} . It is found that the amide oxygen

(6) Zollner, H. *In Handbook of Enzyme Inhibitors*; VCH: Weinheim, Germany, 1993; Part A, pp 33-43.

(7) Kitson, T. M. *Biochem. J.* **1991**, *278*, 189 and refs cited therein.

(8) Sarges, R.; Schnur, R. C.; Belletire, J. L.; Peterson, M. J. *J. Med. Chem.* **1988**, *31*, 230.

(9) Mylari, B. L.; Larson, E. R.; Beyer, T. A.; Zembrowski, W. J.; Aldinger, C. E.; Dee, M. F.; Siegel, T. W.; Singleton, D. H. *J. Med. Chem.* **1991**, *34*, 108.

(10) Kapmeyer, H.; Pfeiderer, G.; Trommer, W. E. *Biochemistry* **1976**, *15*, 5024.

(11) (a) Almarsson, Ö.; Karaman, R.; Bruice, T. C.; *J. Am. Chem. Soc.* **1992**, *114*, 8702. (b) Almarsson, Ö.; Bruice, T. C.; *J. Am. Chem. Soc.* **1993**, *115*, 2125.

(12) Tapia, O.; Cardenas, R.; Colonna-Cesari F. *J. Am. Chem. Soc.* **1988**, *110*, 4046.

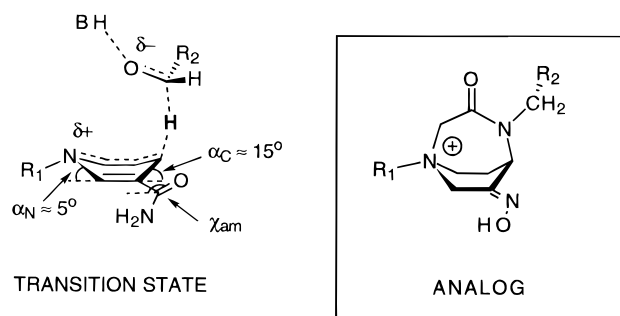
(13) Wu, Y.-D.; Houk, K. N. *J. Am. Chem. Soc.* **1987**, *109*, 2226.

(14) Wilkie, J.; Williams, I. H. *J. Am. Chem. Soc.* **1992**, *114*, 5423.

(15) Wu, Y.-D.; Lai, D. K. W.; Houk, K. N. *J. Am. Chem. Soc.* **1995**, *117*, 4100.

(16) (a) Deng, H.; Zheng, J.; Sloan, D.; Burgner, J.; Callender, R. *Biochemistry* **1992**, *31*, 5085. (b) Deng, H.; Burgner, J.; Callender, R. *J. Am. Chem. Soc.* **1992**, *114*, 7997.

Scheme 2. Calculated Transition State Geometry for Hydride Transfer and the Proposed Analog



TRANSITION STATE

ADH enzyme
(R₁ = ADP-ribosyl, R₂ = CH₃)catalytic antibody
(R₁ = CH₂C₆H₄CONH(CH₂)₂OH,
R₂ = alkyl)

is trans to C(2) in enzyme–NAD complexes ($\chi_{am} = \pm 160^\circ$) and that an out-of-plane orientation lowers the transition state energy and thereby directs the stereospecificity of hydride transfer.¹⁷ Finally the torsion angle around the C–N bond between the ribose and the nicotinamide χ_n may adopt either an *anti* (A-specific dehydrogenases, $-170^\circ < \chi_n < -80^\circ$) or a *syn* orientation (B-specific dehydrogenases, $43^\circ < \chi_n < 86^\circ$)¹⁸ and is correlated with the redox potential of the substrates for a number of dehydrogenases.¹⁹

Design of the Transition State Analog. We chose to construct a transition state analog for the hydride transfer between **4** and an aliphatic aldehyde (Scheme 1). The choice of **4** instead of the natural cofactor NADH would allow us to distinguish specific antibody catalysis from contaminant dehydrogenases in antibody cell cultures and was supported by model studies on the redox properties of *N*-alkylnicotinamide derivatives showing that such compounds behave similarly to the naturally occurring cofactor NAD.²⁰

We envisioned that a rigid analog closely matching the transition state could be realized by installing a lactam bridge between position 1 and 4 of 3-piperidone oxime (Scheme 2). This lactam bridge enforced the reactive boat conformation on the pyridine ring while simultaneously providing an anchor for the aliphatic chain of an aldehyde substrate at the appropriate site in the form of the lactam nitrogen. In addition, the oxygen atom of the carbonyl was properly positioned to serve as a polar mimic for the carbonyl oxygen of the aldehyde. Quaternization of the piperidine nitrogen would install a permanent positive charge in agreement with the partial charge of that atom at the transition state. This positive charge would also induce the key general acid–base residue (BH in Scheme 2) in the antibody upon immunization.²¹ Hydrogen-bonding of this catalytic residue

(17) (a) Donkersloot, M. C. A.; Buck, H. M. *J. Am. Chem. Soc.* **1981**, *103*, 6554. (b) de Kok, P. M. T.; Bastiaansen, L. A. M.; van Lier, P. M.; Vekemans, J. A. J.M.; Buck, H. M. *J. Org. Chem.* **1989**, *54*, 1313.

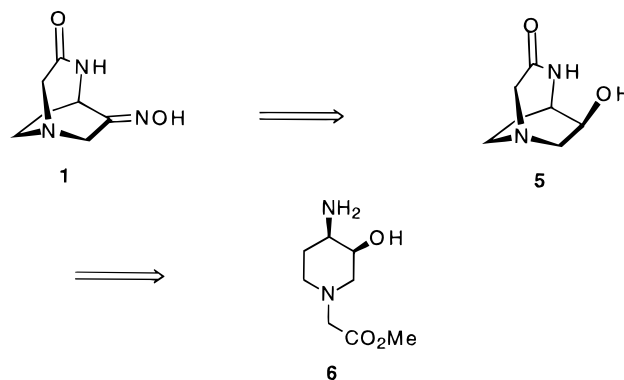
(18) Wu, Y.-D.; Houk, K. N. *J. Am. Chem. Soc.* **1991**, *113*, 2353.

(19) Benner, S. A.; Nambiar, K. P.; Chambers, G. K. *J. Am. Chem. Soc.* **1985**, *107*, 5513.

(20) (a) Mauzerall, D.; Westheimer, F. H. *J. Am. Chem. Soc.* **1955**, *77*, 2261. (b) Ohnishi, Y.; Tanimoto, S. *Tetrahedron Lett.* **1977**, *22*, 1909. (c) Johnston, C. C.; Gardner, J. L.; Suelter, C. H.; Metzler, D. E. *Biochemistry* **1963**, *2*, 689. (d) Kim, C. S. Y.; Chaykin, S. *Biochemistry* **1968**, *7*, 2339. (e) van Eikeren, P.; Grier, D. L.; Eliason, J. *J. Am. Chem. Soc.* **1979**, *101*, 7402. (f) Ohno, A.; Ushida, S.; Oka, S. *Bull. Chem. Soc. Jpn.* **1984**, *57*, 506. (g) Ohnishi, Y. *Tetrahedron Lett.* **1977**, 2109.

(21) Koch, T.; Reymond, J.-L.; Lerner, R. A.; *J. Am. Chem. Soc.* **1995**, *117*, 9383 and refs cited therein.

Scheme 3. Retrosynthesis of Transition State Analog 1



with the lactam carbonyl might provide a spatial arrangement favorable for catalysis.

Replacement of the three olefinic CH groups of the dihydropyridine group in the transition state by aliphatic methylenes in the analog was necessary to obtain a synthetically feasible structure. This replacement was judged acceptable since the van der Waals volume and polarity of both groups are quite similar. However, molecular modeling showed that unless at least one sp²-center was maintained on the piperidine ring corresponding to the dihydropyridine, the symmetrical boat conformation corresponding to the transition state would flip to a strongly tilted twist–boat conformation in the bicyclic analog (see below, Figure 1B). The required sp²-center was introduced in the form of an oxime as a replacement for the carboxamide group at position 3 of the dihydropyridine. Despite of the fact that the orientation of the carboxamide at the transition state ($\chi_{am} = \pm 160^\circ$, see above) was not programmed by this replacement, the oxime would induce a polar, hydrogen-bonding environment capable of accommodating the carboxamide substituent of the dihydropyridine cofactor. This led to the bicyclic lactam **1** (Chart 1) as the primary synthetic target.

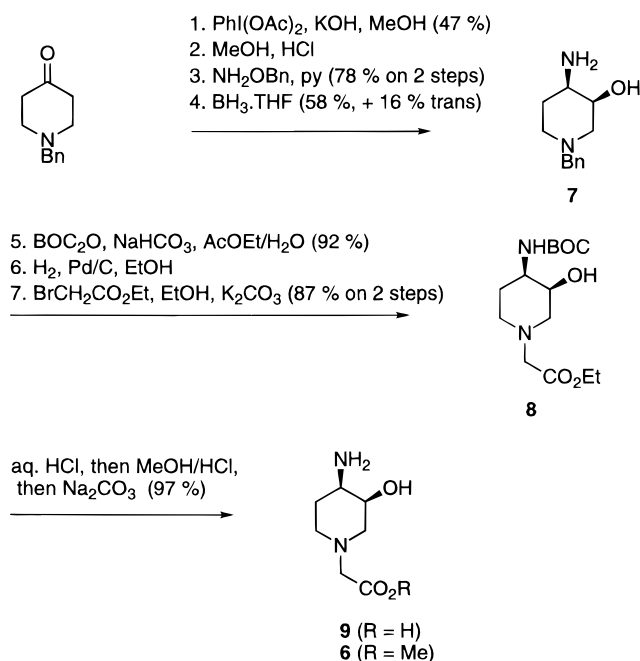
Derivatives **2** and **3** were planned as haptens for conjugation to carrier proteins and immunization, to generate catalytic antibodies for the reduction of simple aliphatic aldehydes by the 1,4-dihydropyridine **4** (Scheme 1). The aldehyde carbon in the transition state was mimicked by a methylene group in hapten **2**. Alternatively, this carbon was mimicked by a sulfonyl group in hapten **3**, thereby providing two additional oxygen atoms as mimics for the carbonyl oxygen in orientations compatible with the overall geometry of the process. These might enable additional H-bonding residues to be induced in the antibodies during the immune response.

Synthesis. In the retrosynthetic analysis of target lactam **1**, the oxime function would derive from secondary alcohol **5**, which could be obtained by cyclization from piperidine precursor **6** (Scheme 3).

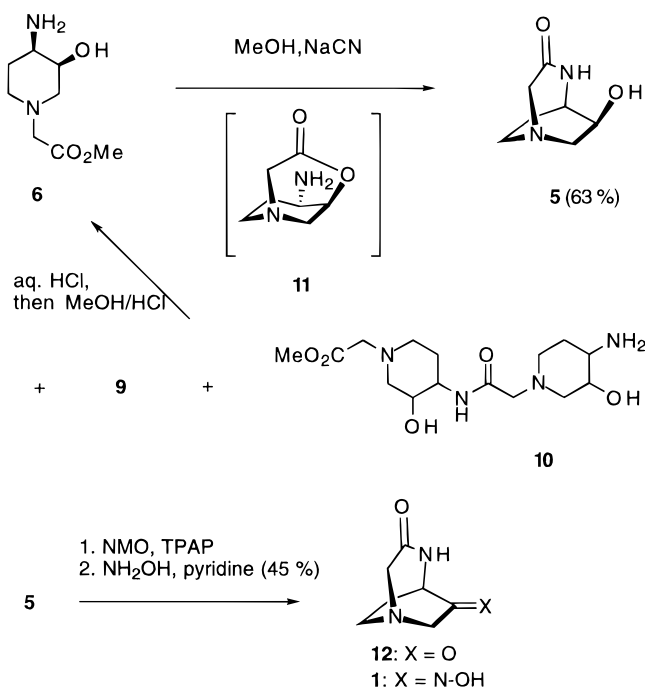
cis-aminohydroxypiperidine **7** was prepared from *N*-benzylpiperidone following published procedures (Scheme 4).²² BOC protection of the primary amine followed by debenylation and alkylation of the piperidine nitrogen with ethyl bromoacetate gave **8**. Removal of the BOC group under standard conditions (CF₃COOH in CH₂Cl₂ or TMSCl–phenol in CH₂Cl₂)²³ gave very low yield, presumably due to formation of an urethane with the

(22) Ghosh, A. K.; McKee, S. P.; Sanders, W. M. *Tetrahedron Lett.* **1991**, *32*, 711.

Scheme 4. Synthesis of Amino Alcohol 6



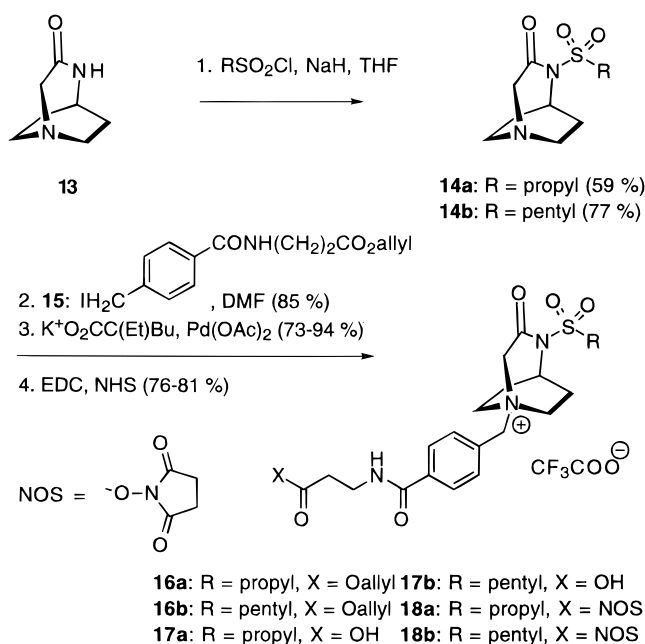
Scheme 5. Synthesis of Compound 1



adjacent hydroxyl group. Quantitative conversion of **8** to **6** was accomplished by hydrolysis in aqueous HCl to the corresponding amino acid **9**, followed by reesterification in methanolic HCl.

Treatment of **6** in refluxing anhydrous methanol with catalytic potassium cyanide gave the bicyclic alcohol **5**, which was isolated in 63% yield (Scheme 5). Dimer **10** (mixture of stereoisomers), amino acid **9**, and starting material were obtained as side products and recycled to **6** by acidic hydrolysis and reesterification. Attempts to cyclize the *trans*-amino alcohol corresponding to **6** gave only small amounts of dimer, suggesting that the intramolecular cyclization to **5** was facilitated by formation

Scheme 6. Synthesis of Model Compounds 17a/b



of the bicyclic intermediate **11**. Alcohol **5** was then oxidized with *N*-methylmorpholine oxide (NMO) and catalytic tetrapropylammonium perruthenate²⁴ (TPAP) in DMF/acetonitrile to give ketone **12**. This ketone was highly sensitive to hydrolysis in contact with silica gel and was directly converted to the stable oxime **1** by treatment with excess hydroxylamine in pyridine.²⁵

Functionalization of compound **1** was first explored starting from amide **13**, easily prepared by Beckman rearrangement of quinuclidone oxime (Scheme 6).²⁶ Alkylation of the bridge amide nitrogen with propanesulfonyl chloride or pentanesulfonyl chloride yielded sultams **14a** and **14b**, which were alkylated with iodide **15** to ammonium salts **16a** and **16b**. Protection of the carboxyl function in **15** was required due to polymerization of the free acid during the reaction. Cleavage of the allyl ester under neutral and nonreducing conditions was achieved using potassium 2-ethyl hexanoate and palladium acetate.²⁷ The resulting free acids **17a** and **17b** were finally converted to the corresponding *N*-hydroxysuccinimide esters **18a** and **18b** with EDC (3-(*N*-ethyl-*N*-diethylamino)propylcarbodiimide) in aqueous DMF.

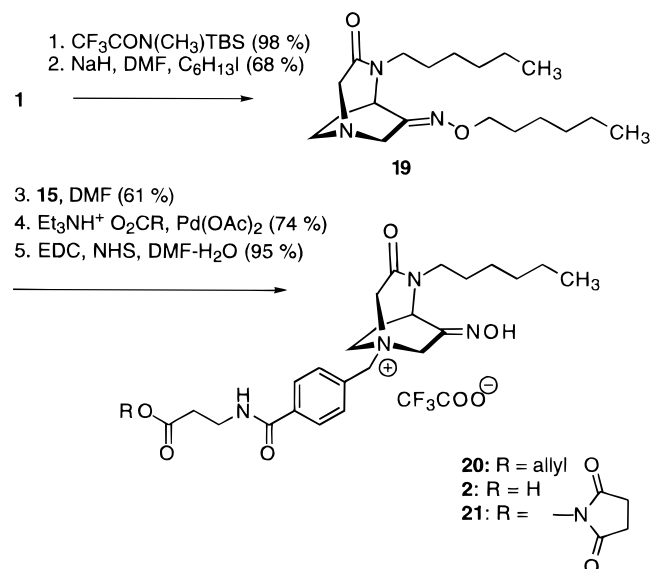
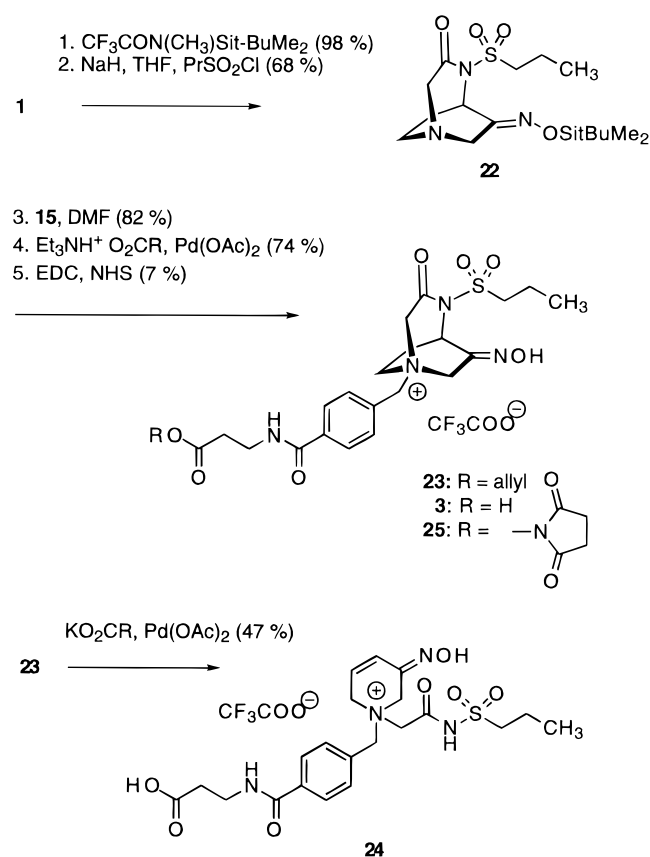
Compound **1** was similarly functionalized to haptens **2** and **3** (Scheme 7). Despite protection of the oxime, alkylation with iodoheptane gave the double alkylated derivative **19**. Fortunately, quaternization with iodide **15** led to quaternary ammonium salt **20**, in which the oxime hexyl substituent had been removed, presumably by nucleophilic substitution with iodide in analogy to known ether and ester cleavage procedures.²⁸ Cleavage of the allyl ester as above gave **2**, which was then converted to an activated *N*-hydroxysuccinimide ester **21** and conjugated to carrier proteins KLH (keyhole limpet hemocyanin) and BSA (bovine serum albumin) for immunizations.

(24) Ley, S. V.; Norman, J.; Griffith, W. P.; Marsden, S. P. *Synthesis* **1994**, 639.

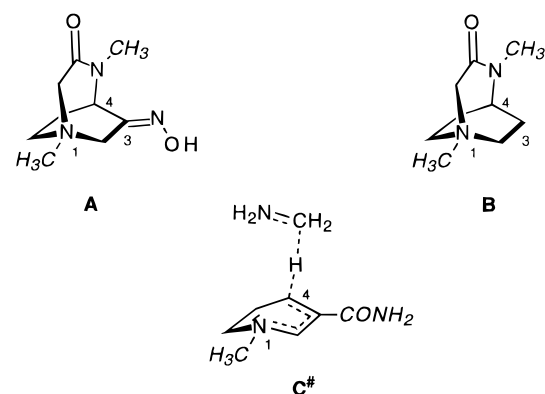
(25) Sternbach, L. H.; Kaiser, S. *J. Am. Chem. Soc.* **1952**, *74*, 2215.
 (26) Rubsov, M. V.; Mikhлина, E. E.; Vorob'eva, V. Y.; Yanina, A. D. *J. Gen. Chem.* **1964**, *34*, 2232.

(27) Jeffrey, P. D.; McCombie, S. W. *J. Org. Chem.* **1982**, *47*, 587.
 (28) Bhatt, M. V.; El-Morey, S. S. *Synthesis* **1982**, 1048.

(23) Kaiser, E., Sr.; Tam, J. P.; Kubiak, T. M.; Merrifield, R. B. *Tetrahedron Lett.* **1988**, *29*, 303.

Scheme 7. Functionalization of 1 to Hapten 2**Scheme 8. Functionalization of 1 to Hapten 3**

Sulfonylation of silylated **1** using propanesulfonyl chloride gave sultam **22** without loss of the oxime silyl group (Scheme 8). Reaction with iodide **15** as above followed by deprotection of the silyl group with aqueous acid gave the quaternary ammonium salt **23**. Deprotection of the allyl group using triethylammonium 2-ethylhexanoate under palladium catalysis gave hapten **3**. Interestingly, an attempted deprotection using the more basic potassium 2-ethylhexanoate and palladium gave the ring-opened product **24**, resulting from elimination of the sultam group. Hapten **3** and its derivatives were highly sensitive to aqueous basic conditions due to hydrolysis of the bridge sultam. Nevertheless it was

Chart 3. Structure of Models A, B, and C#^a

^a Substituents added or modified for modeling purposes are in italics.

possible to obtain the activated ester **25** in moderate yield and prepare conjugates with carrier protein KLH and BSA as above.

Structural Comparisons between Transition State and Its Analogs

Suitable crystals could be obtained for compounds **1** and **17b** and their structure determined by X-ray crystallography. As model for the corresponding transition state we selected Houk's transition state for hydride transfer between 1,4-dihydropyridine and the methylene imminium cation.¹³

For comparison purposes the substitution patterns of both analogs and the transition state were unified. As common replacement for either the ribosyl or the benzyl substituent, a methyl substituent was attached to the bridgehead nitrogen in **1** and **17b** and to the dihydropyridine N(1) nitrogen in the calculated transition state. A methyl group was also attached to the bridge lactam nitrogen in **1** and **17b** as a match for the carbon of the methylene imminium cation in the transition state, leading to model structure **A** from **1** and **B** from **17b** (Chart 3). Finally a carboxamide substituent was attached to C(3) of the dihydropyridine in the transition state, with the oxygen trans to C(2) ($\chi_{\text{am}} = 160^\circ$), as seen in dehydrogenase-NAD complexes, leading to transition state model **C#**. These modifications were performed using the modeling package "Insight" from Biosym.

An atom-by-atom superimposition of model **A** (from **1**) and the transition state **C#** is shown in Figure 1A and illustrates the close similarities between the two structures.²⁹ The boat conformation of the dihydropyridine mimic in model **A** is too strongly puckered compared to the transition state. However the bicyclic arrangement allows one to place the substrate carbonyl mimic, represented by the *N*-methyl substituent and the oxygen of the bridge lactam, in the correct position above the pyridine ring. In addition, the oxime substituent at C(3) has an excellent overlap with the carboxamide substituent in the transition state.

This oxime substituent at C(3) also plays a further role in controlling conformation. The piperidine ring in **A** adopts a symmetrical boat conformation mimicking the

(29) Upson, C.; Faulhaber, T.; Kamins, D.; Laidlaw, D.; Schlegel, D.; Vroom, J.; Gurwitz, R.; vanDam, A. *IEEE Comput. Graphics Appl.* **1989**, 9, 30–42.

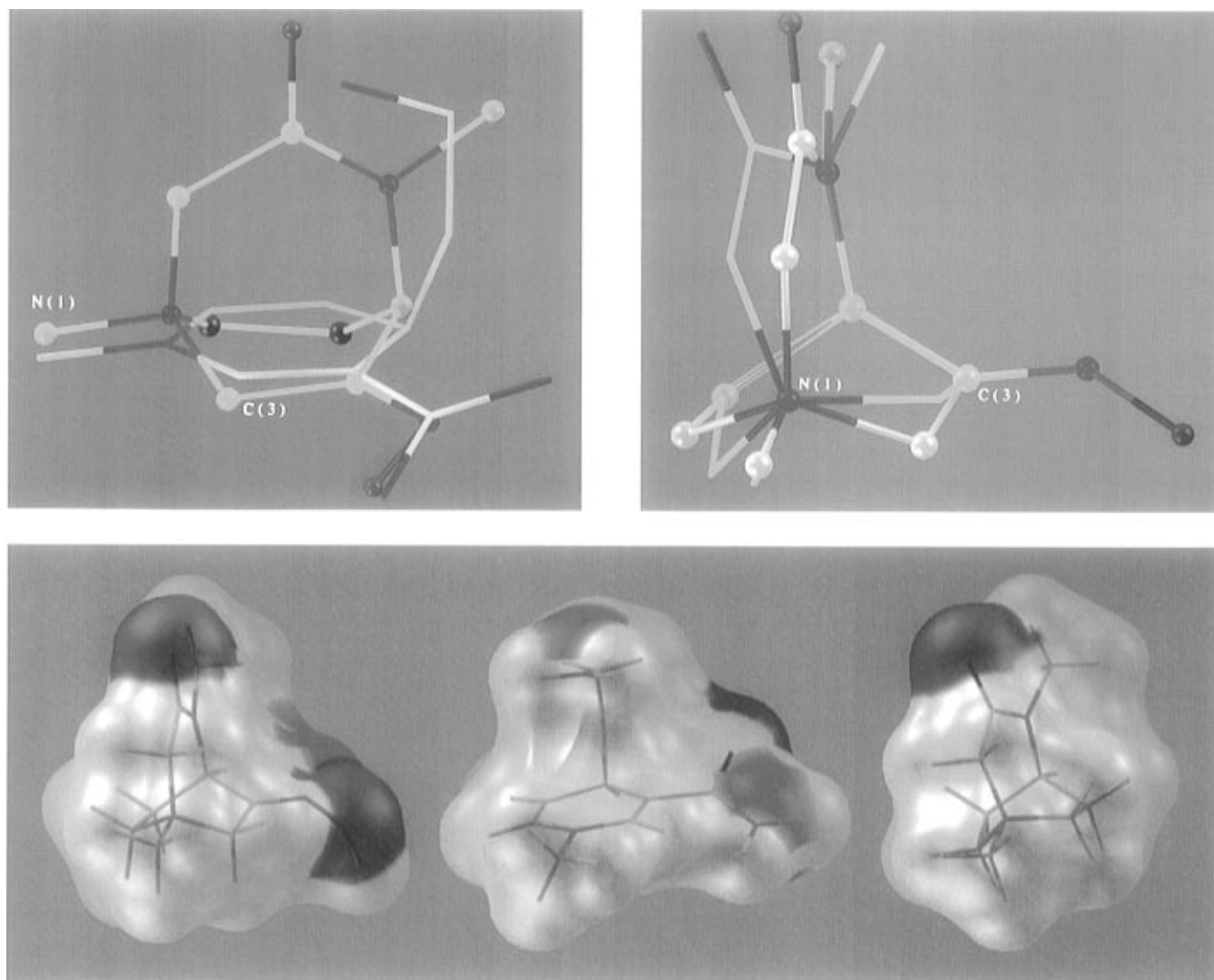


Figure 1. (A, Top left) superimposition of model **A** (green), derived from the X-ray coordinates of **1**, and model **C[#]** (white), derived from the calculated transition state for hydride transfer. All atoms in the transition state **C[#]**, except the hydrogen atom and the oxygen atom of the carboxamide substituent at C(3), were used in the superimposition. The pictures in parts A–C were rendered on a Dec Alpha with a Denali graphics board using the AVS graphics software. (B, Top right) superimposition of models **A** (white) and **B** (green), derived from the X-ray coordinates of **1** and **17b**. Atoms N(1), C(3), and C(4) were used in the superimposition. The sp^2 hybridization of C(3) allows for a symmetrical boat conformation in **A** which fits the transition state **C[#]** (see part A). The simpler model **B** with an sp^3 hybridization at C(3) adopts a twist-boat conformation which also brings the three-atom bridge out of symmetry. (C, Bottom) solvent-excluded surfaces of models **A** (left, derived from the X-ray coordinates of **1**), **B** (right, derived from the X-ray coordinates of **17b**), and **C[#]** (center, derived from the calculated transition state for hydride transfer) using the program MSMS.²⁹ The surfaces are colored according to atom type: carbon or hydrogen in white, oxygen in red, nitrogen in blue. Model **A** mimicks nicely the shape and polarity of transition state **C[#]**.

dihydronicotinamide in **C[#]**. As shown by a superimposition of models **A** and **B** (Figure 1B), the piperidine ring in **B**, which lacks this substituent, adopts a strongly tilted twist-boat conformation. This tilted conformation in **B** also displaces the three-atom lactam bridge out of symmetry, leading to further dissimilarity between **B** and **C[#]**.

The solvent-excluded surface of each model is shown in Figure 1C. The surfaces were calculated using the program MSMS.³⁰ The surface are colored according to atom type to distinguish nonpolar surfaces induced by hydrocarbon parts of the structures (white) from polar surfaces with hydrogen-bonding capacity with oxygen (red) or nitrogen (blue). Such distinction is meaningful with respect to the planned interactions with an antibody-

binding pocket in an aqueous environment, where hydrophobic and hydrogen-bonding interactions are key determinants of the binding energy.³¹ While model **B** (right in Figure 1C) is clearly not a suitable analog of **C[#]** (center in Figure 1C), the molecular surfaces of **A** (left in Figure 1C) and **C[#]** are quite similar. Here again the oxime substituent at C(3) plays a key role in providing model **A** with an overall shape similar to that of transition state **C[#]**. By its volume and polarity, this oxime is an excellent match for the carboxamide substituent at C(3) of dihydronicotinamide.

(31) We have not used electrostatic potential comparisons between analog and transition state because several examples in the literature (the "bait and switch" strategy, where a positively charged transition state analog mimics a negatively charged transition state, cited in ref 2b) are in clear contradiction with the notion that close electrostatic analogy is a condition for inducing catalytic antibodies.

(30) Sanner, M.; Olson, A.; Spehner, J. C. *Biopolymers* **1996**, *38*, 305.

Conclusion

The design and synthesis of an accurate and conformationally stable transition state analog for the alcohol dehydrogenase reaction have been reported. This transition state analog possesses a rigid bicyclic structure that presents all crucial elements of the transition state for hydride transfer in the appropriate geometry. Compound **1** was readily prepared in 10 steps from *N*-benzylpiperidone and functionalized to haptens **2** and **3** and their carrier protein conjugates. These conformationally rigid analogs present an excellent structural fit to the transition state for hydride transfer both in terms of shape and polarity. The production of monoclonal antibodies against these haptens and their characterization for catalysis will be reported separately.

Experimental Section

Reagents were purchased from Aldrich or Fluka. Solvents were A.C.S. grade from Fisher. All chromatographies (flash) were performed with Merck Silica gel 60 (0.040–0.063 mm). Preparative HPLC was done with Fisher Optima grade acetonitrile and ordinary deionized water using a Waters prepak cartridge (500 g) installed on a Waters Prep LC 4000 system from Millipore, (flow rate 100 mL/min, gradient +0.5%/min CH₃CN, detection by UV at 254 nm). TLC analyses were performed with fluorescent F254 glass plates. MS, HRMS, and combustion analyses were provided by the Scripps Research Institute facility (Gary Szuidak). X-ray crystallography was performed by Dr. Raj K. Chadha at Scripps.

tert-Butyl (3'*RS*,4'*SR*)-*N*-(1'-((Ethoxycarbonyl)methyl)-3'-hydroxypiperidin-4'-yl)carbamate (8). A solution of amino alcohol **7** (6.14 g, 29.8 mmol) in ethyl acetate/water (each 80 mL) containing sodium hydrogen carbonate (7.50g, 89.3 mmol) and di-*tert*-butyl dicarbonate (10.8g, 49.6 mmol) was stirred vigorously for 15 h at 25 °C. The phases were separated, and the product obtained upon evaporation of the organic phase was purified by flash chromatography (hexane/acetone 3:1, *R*_f = 0.25) to yield the *N*-BOC derivative of **7** (8.37g, 92%). This compound (8.37 g, 27.3 mmol) was dissolved in 96% ethanol (200 mL) and vigorously stirred with a catalytic amount of palladium hydroxide (10% on charcoal) under 1 atm of hydrogen for 16 h at 25 °C. The catalyst was filtered off over Celite, and the filtrate was concentrated to 100 mL and refluxed for 16 h in the presence of ethyl bromoacetate (3.6 mL, 5.4 g, 32 mmol) and sodium hydrogen carbonate (3.467 g, 41.27 mmol). Solvent removal in vacuo, aqueous workup (aqueous NaCl/CH₂Cl₂), and flash chromatography (hexane/acetone 3:1, *R*_f = 0.20) gave **8** as colorless solid. Mp: 77–78 °C (7.19 g, 87%).

¹H-NMR (300 MHz, CDCl₃): 5.00 (d, 1H, *J* = 8.8); 4.13 (q, 2H, *J* = 7.2); 3.74 (br s, 1H); 3.48 (m, 1H); 3.21 (2, 2H); 2.92 (ddd, 1H, *J* = 11.7, 3.6, 2.5); 2.78 (dq, 1H, *J* = 9.6, 2.5); 2.50 (d, 1H, *J* = 11.7); 2.35 (td, 1H, *J* = 11.7, 3); 1.77 (m, 1H); 1.67 (qd, 1H, *J* = 11.7, 4.5); 1.40 (s, 9H); 1.24 (t, 3H, *J* = 7.2). HRMS: C₁₄H₂₆N₂O₅ (M + H⁺) calcd 303.1920, found 303.1925. IR (CCl₄): 3446, 2979, 1743, 1713, 1495, 1178. Anal. Calcd: C, 55.61; H, 8.67; N, 9.26. Found: C, 55.55; H, 8.81; N, 9.08.

(3*RS*,4*SR*)-*N*-(Methoxycarbonyl)methyl)-4-amino-3-hydroxypiperidine (6). A solution of **8** (7.65 g, 25.3 mmol) in 200 mL of 3 N aqueous HCl was heated to 80 °C for 16 h. The hydrochloric acid was removed in vacuo, and the residue was taken up in absolute methanol (200 mL). After addition of 3 Å molecular sieve (6 g), the solution was saturated with hydrogen chloride gas and refluxed for 5 h. The solvent was removed in vacuo and the white solid residue dissolved in water (150 mL). The solution was adjusted with aqueous sodium carbonate to pH 8. Extraction with ethyl acetate and chromatography (CH₂Cl₂/MeOH/aqueous NH₃ 5:1:0.2, *R*_f = 0.40) gave **6** as colorless liquid (4.63 g, 97%). ¹H-NMR (500 MHz, CDCl₃): 3.69 (br s, 1H); 3.59 (s, 3H); 3.56 (br s, 1H); 3.18, 3.14 (2d, 2 × 1H, *J* = 17); 2.80 (br d, 1H, *J* = 12); 2.74–2.65 (m, 1H); 2.41 (br d, 1H, *J* = 12); 2.26 (td, 1H, *J* = 11, 3);

1.70–1.56 (m, 2H). ¹³C-NMR (125 MHz, CDCl₃): 170.9, 67.7, 58.3, 57.1, 51.3, 50.7, 28.8. HRMS: C₈H₁₆N₂O₃ (M + H⁺) calcd 189.1239, found 189.1241. IR (CDCl₃): 3373, 2952, 2252, 1739, 1653, 1203.

1,4-Diaza-6-hydroxybicyclo[3.2.2]nonan-3-one (5). A solution of amino alcohol **8** (0.497 g, 2.64 mmol) and sodium cyanide (0.0135 g, 0.276 mmol) in anhydrous methanol (50 mL) over molecular sieve (3 Å, 3 g) was refluxed for 3 h. The molecular sieve was filtered off and the methanol evaporated in vacuo. The residue was dissolved in a small amount of methanol and rapidly filtered through a silical gel plug (CH₂Cl₂/MeOH/aqueous NH₃ 7:1:0.2; TLC 3:1:0.3, *R*_f = 0.25) to give **5** as a colorless crystalline product. Mp: 237–238 °C (subl) (0.26 g, 63%). Small amounts of **6** were removed by washing the solid extensively with ethyl acetate. Dimer **10** (*R*_f = 0.42) and amino acid **9** (CH₂Cl₂/MeOH/aqueous NH₃ 3:2:1, *R*_f = 0.4) were obtained as side products. These were recycled to starting material **6** by hydrolysis in 3 N hydrochloric acid followed by esterification with methanol. ¹H-NMR (300 MHz, CD₃OD): 4.00 (td, 1H, *J* = 4.5, 8); 3.63 (br s, 2H); 3.36 (m, 1H); 3.30 (m, 1H); 3.03–2.86 (m, 2H); 2.71 (ddd, 1H, *J* = 14.6, 4.4, 2.1); 2.22 (dddd, 1H, *J* = 14.5, 8.9, 6.3, 2.5); 1.92 (dddd, 1H, *J* = 19.3, 5.2, 3.8, 1.0).

¹³C-NMR (125 MHz, CD₃OD): 180.7, 72.0, 64.8, 58.4, 52.6, 48.1, 31.8. HRMS: C₇H₁₂N₂O₂ (M + H⁺) calcd 157.0977, found 157.0979. IR (KBr): 3397, 2907, 2861, 2461, 2265, 1597, 1466, 1351, 1087, 1052. Anal. Calcd: C, 53.83; H, 7.74; N, 17.94. Found C, 53.74; H, 7.88; N, 17.86.

Dimer **10**: ¹H-NMR (300 MHz, CDCl₃): 7.74, 7.58 (2 d, 1H, *J* = 9); 3.95–3.80 (m, 1H); 3.76 (br s, 2H); 3.70 (s, 3H); 3.20 (m, 2H); 3.15–2.60 (m, 11 H); 2.55 (m, 1H); 2.40–2.15 (m, 3H); 1.85–1.62 (m, 4H). MS (electrospray): (M + H⁺) 345, (M + Na⁺) 367.

Amino acid **9**: ¹H-NMR (300 MHz, D₂O): 3.80 (br s, 1H); 3.08 (dd, 1H, *J* = 16.7, 11.7, 8.5); 2.98 (s, 2H); 2.91 (br d, 1H, *J* = 13); 2.78 (br d, 1H, *J* = 12); 2.43 (dd, 1H, *J* = 13, 1); 2.27 (td, 1H, *J* = 11.7, 3.1); 1.78 (ddd, 1H, *J* = 13.3, 11.4, 4.1); 1.67 (ddd, 1H, *J* = 13, 9, 4). MS (FAB): (M + H⁺) 175.

1,4-Diaza-6-(hydroxylimino)bicyclo[3.2.2]nonan-3-one (1). Tetrapropylammonium perruthenate (0.33 g, 0.95 mmol) was added to a suspension of **5** (1.0 g, 6.4 mmol), *N*-methylmorpholine *N*-oxide (1.22 g, 10.4 mmol), and powdered molecular sieve (4 Å, 6.5 g) in acetonitrile/*N,N*-dimethylformamide 1:1 (30 mL). This mixture was stirred at 25 °C for 4 h. The acetonitrile was evaporated and the residue was rapidly passed through a plug of silica gel (CH₂Cl₂/MeOH 4:1, TLC CH₂Cl₂/MeOH/aqueous NH₃ 4:1:0.3, *R*_f = 0.4). The product-containing fractions were evaporated and dried for several minutes in vacuo. The sensitive colorless crystalline ketone **12** was then dissolved in pyridine/ethanol 3:2 (25 mL) and stirred at 25 °C for 16 h with molecular sieves (4 Å, 2 g) and hydroxylamine hydrochloride (0.92 g, 13.2 mmol). The molecular sieves were filtered off, and the solvents were evaporated in vacuo. The residue was purified by chromatography (methylene chloride/methanol/aqueous NH₃ 7:1:0.15; TLC, CH₂Cl₂/MeOH/aqueous NH₃ 4:1:0.25, *R*_f = 0.40) to give **1** (0.49 g, 45%) as a crystalline solid. Mp: 259–260 °C (dec.). ¹H-NMR (300 MHz, D₂O): 3.82 (dd, 1H, *J* = 5, 2); 3.80, 3.70 (2d, 2 × 1H, *J* = 19); 3.62, 3.52 (2d, 2 × 1H, *J* = 19); 3.05–2.80 (m, 2H); 2.32 (m, 1H); 2.00 (dddd, 1H, *J* = 20, 15, 10, 5). ¹³C-NMR (125 MHz, D₂O): 179.1, 161.6, 62.0, 50.9, 49.2, 47.1, 31.7. MS (FAB+): (M + H⁺) 170. IR (KBr): 3422, 2345, 1654, 1636, 1324, 1137, 931. Anal. C₇H₁₁N₃O₂ Calcd: C, 49.70; H, 6.55; N, 24.83. Found C, 49.47; H, 6.83; N, 25.11.

1,4-Diaza-4-(propylsulfonyl)bicyclo[3.2.2]nonan-3-one (14a) and 1,4-Diaza-4-(pentylsulfonyl)bicyclo[3.2.2]nonan-3-one (14b). Sodium hydride (60% in mineral oil, 0.12 g, 3.0 mmol) was added to a suspension of **13** (0.20 g, 1.43 mmol) in tetrahydrofuran (20 mL). After 1 h at 25 °C 1-propanesulfonyl chloride (0.60 mL, 5.3 mmol) was added slowly. The reaction was quenched after 2 h with acetic acid (0.2 mL). The solvent was removed in vacuo, and the residue was purified by chromatography (CH₂Cl₂/MeOH/aqueous NH₃ 10:1:0.1, *R*_f = 0.40) to give sultam **14a**, a colorless solid. Mp: 58–59 °C (0.208 g, 59%). ¹H-NMR (500 MHz, CDCl₃): 4.57 (m, 1H); 3.72 (s, 2H); 3.44 (m, 2H); 3.02 (m, 2H); 2.92 (m, 2H);

2.06–1.92 (m, 4H); 1.70 (m, 2H); 0.98 (t, 3H, $J = 7.5$). ^{13}C -NMR (125 MHz, CDCl_3): 176.9, 62.7, 56.0, 47.7, 45.2, 28.5, 16.9, 12.5. HRMS: $\text{C}_{10}\text{H}_{18}\text{N}_2\text{O}_3\text{S}$ ($\text{M} + \text{Cs}^+$) calcd 379.0092, found 379.0096. IR (CCl_4): 2938, 2878, 1681, 1355, 1249, 1150. Anal. Calcd: C, 48.76; H, 7.37; N, 11.37; S, 13.02. Found C, 48.62; H, 7.65; N, 11.48; S, 12.77.

A similar procedure using pentanesulfonyl chloride gave sultam **14b** ($R_f = 0.40$), a waxy solid. Mp: 23–24 °C (0.302 g, 77%). ^1H -NMR (500 MHz, CDCl_3): 4.62 (m, 1H); 3.77 (s, 2H); 3.50 (m, 2H); 3.06 (m, 2H); 2.97 (m, 2H); 2.07 (m, 2H); 2.00 (m, 2H); 1.69 (m, 2H); 1.40–1.28 (m, 4H); 0.86 (t, 3H, $J = 7.5$). ^{13}C -NMR (125 MHz, CDCl_3): 177.0, 62.8, 54.4, 47.7, 45.2, 29.8, 28.6, 22.7, 21.9, 13.5. HRMS: $\text{C}_{12}\text{H}_{22}\text{N}_2\text{O}_3\text{S}$ ($\text{M} + \text{Cs}^+$) calcd 407.0405, found 407.0409. IR (CCl_4): 2957, 2875, 1683, 1354, 1249, 1150. Anal. Calcd: C, 52.53; H, 8.08; N, 10.21; S, 11.68. Found C, 52.24; H, 8.48; N, 10.07; S, 12.20.

***N*-(2'-((Allyloxy)carbonyl)ethyl)-4-(iodomethyl)benzamide (15)**. A suspension of β -alanine (1.50 g, 16.9 mmol) in allyl alcohol (12 mL) was saturated with gaseous hydrogen chloride and stirred for 1 h at 25 °C. Removal of the solvent in vacuo yielded β -alanine allyl ester hydrochloride (2.77 g, 99%) as a colorless solid. A suspension of 4-(chloromethyl)benzoic acid (3.62 g, 21.2 mmol) in 100 mL of CH_2Cl_2 and *N,N*-dimethylformamide (10 drops) was treated with oxalyl chloride (4.0 mL, 47 mmol) at 25 °C until complete dissolution. Then the solvent and excess reagent were removed in vacuo, and the residue was dissolved in dry methylene chloride (50 mL). Triethylamine (6.0 mL, 43 mmol) and β -alanine allyl ester hydrochloride (2.77 g, 16.7 mmol) were added slowly at 0 °C, and the mixture was stirred for 1 h at 25 °C. Aqueous workup ($\text{NaCl}/\text{Na}_2\text{CO}_3$) and purification by chromatography (hexane/acetone 3:1, $R_f = 0.15$) gave *N*-(2'-((allyloxy)carbonyl)-ethyl)-4-(chloromethyl)benzamide as a colorless crystalline product. Mp: 55–56 °C (4.24 g, 90% over all steps). A solution of this chloride (0.50 g, 1.78 mmol) and sodium iodide (2.22 g, 14.8 mmol) in acetone (18 mL) was refluxed for 2 h. Removal of the solvent in vacuo, aqueous workup (aqueous sodium sulfite/ CH_2Cl_2), and flash chromatography (hexane/acetone 5:2, $R_f = 0.30$) gave **15**. Mp: 100–101 °C (0.5908 g, 89%). ^1H -NMR (300 MHz, CDCl_3): 7.67, 7.40 (2d, 2 × 2H, $J = 8.5$); 6.81 (br t, 1H, $J = 5.8$); 5.90 (ddt, 1H, $J = 17, 10.5, 5.8$); 5.31 (dq, 1H, $J = 17, 1.5$); 5.24 (dq, 1H, $J = 10.5, 1.5$); 4.60 (dt, 2H, $J = 5.8, 1.5$); 4.44 (s, 2H); 3.70 (q, 2H, $J = 5.8$); 2.66 (t, 2H, $J = 5.8$). HRMS: $\text{C}_{14}\text{H}_{16}\text{NO}_3\text{I}$ ($\text{M} + \text{Cs}^+$) calcd 505.9229, found 505.9235. IR (CCl_4): 3388, 1726, 1546, 1499, 1182. Anal. Calcd: C, 45.06; H, 4.32; N, 3.75. Found C, 45.10; H, 3.95; N, 3.46.

1-((4'-((2-((Allyloxy)carbonyl)ethyl)carbamoyl)phenyl)methyl)-4-aza-3-oxo-4-(propylsulfonyl)bicyclo[3.2.2]nonan-1-azonium Trifluoroacetate (16a) and 1-((4'-((2-((Allyloxy)carbonyl)ethyl)carbamoyl)phenyl)methyl)-4-aza-3-oxo-4-(pentylsulfonyl)bicyclo[3.2.2]nonan-1-azonium Trifluoroacetate (16b). A solution of the sultam **14a** (0.10 g, 0.41 mmol) and iodide **15** (0.23 g, 0.62 mmol) in *N,N*-dimethylformamide (1 mL) was gently heated to 45 °C for 14 h. The reaction mixture was diluted with acetonitrile (5 mL) and water (containing 0.1% trifluoroacetic acid, 40 mL). The precipitate was filtered off and washed with water (5 × 40 mL containing 0.1% trifluoroacetic acid). The filtrate was purified by preparative reverse phase HPLC (see Table 1) to give **16a** as a colorless oil (0.210 g, 85%). ^1H -NMR (300 MHz, CDCl_3): 7.77, 7.56 (2d, 2 × 2H, $J = 8.5$); 7.60 (t, 1H, $J = 6$); 5.90 (ddt, 1H, $J = 17, 10.5, 5.8$); 5.30 (dd, 1H, $J = 17, 1.4$); 5.22 (dd, 1H, $J = 10.5, 1.4$); 4.90 (s, 2H); 4.76 (br s, 1H); 4.73 (s, 2H); 4.58 (dd, 2H, $J = 6, 1$); 3.90 (br s, 4H); 3.69 (q, 2H, $J = 6$); 3.45 (m, 2H); 2.70 (t, 2H, $J = 6$); 2.50–2.28 (m, 4H); 1.75 (hex, 2H, $J = 7.5$); 1.02 (t, 3H, $J = 7.5$). HRMS: $\text{C}_{24}\text{H}_{34}\text{N}_3\text{O}_6\text{S}^+$ (M^+) calcd 492.2168, found 492.2175. IR (CDCl_3): 2253, 1682, 1468, 1381.

A similar procedure starting with sultam **14b** (0.10 g, 0.38 mmol) gave **16b** as a colorless oil (0.202 g, 85%). ^1H -NMR (300 MHz, CDCl_3): 7.72 (m, 3H); 7.51 (m, 2H); 5.89 (ddt, 1H, $J = 17, 10.5, 5.8$); 5.30 (dd, 1H, $J = 17, 1.4$); 5.22 (dd, 1H, $J = 10.5, 1.4$); 4.92 (br s, 2H); 4.75 (br s, 3H); 4.56 (d, 2H, $J = 6$); 3.90 (br s, 4H); 3.67 (q, 2H, $J = 6$); 3.47 (m, 2H); 2.69 (t, 2H, $J = 6$); 2.50–2.10 (m, 4H); 1.68 (m, 2H); 1.42–1.21 (m, 4H);

Table 1. HPLC Conditions for Quaternary Ammonium Derivatives^a

comp	functionality ^b	% A	% B	t_R , min
16a	CO ₂ allyl	40	60	5.4
16b	CO ₂ allyl	30	70	8.2
17a	COOH	60	40	4.1
17b	COOH	40	60	5.4
18a	CO(NOS) ^c	60	40	6.6
18b	CO(NOS)	40	60	8.2
20	CO ₂ allyl	30	70	9.8
2	COOH	30	70	3.9
21	CO(NOS)	30	70	5.6
23	CO ₂ allyl	60	40	5.2
24	COOH	80	20	8.7
3	COOH	60	40	3.6
25	CO(NOS)	60	40	5.4

^a Isocratic elution at 1.5 mL/min; detection by UV at 240 nm; A = 0.1% TFA in H_2O , B = $\text{CH}_3\text{CN}/\text{H}_2\text{O}$ 50:50; analytical column, Microsorb-MV 86–203-C5, 0.45 × 22 cm. Preparative HPLC was performed at 100 mL/min on a Waters prepak cartridge 500 g, gradient +1% B/min starting with 10–15% less B than the isocratic conditions. ^b β -alanine linker. ^c NOS = *N*-oxysuccinimide.

0.86 (t, 3H, $J = 7$). HRMS: $\text{C}_{26}\text{H}_{38}\text{N}_3\text{O}_6\text{S}^+$ (M^+) calcd 520.2481, found 520.2489. IR (CDCl_3): 2932, 2253, 1687, 1549, 1358.

1-((4'-((2-Carbonyl)ethyl)carbamoyl)phenyl)methyl)-4-aza-3-oxo-4-(propylsulfonyl)bicyclo[3.2.2]nonan-1-azonium Trifluoroacetate (17a) and 1-((4'-((2-Carbonyl)ethyl)carbamoyl)phenyl)methyl)-4-aza-3-oxo-4-(pentylsulfonyl)bicyclo[3.2.2]nonan-1-azonium Trifluoroacetate (17b).³² A solution of **16a** (0.100 g, 0.165 mmol) in 2 mL of ethyl acetate was treated with triphenylphosphine (0.25 g, 0.94 mmol), tetrakis(triphenylphosphine)palladium(0) (0.20 g, 0.17 mmol), 2-ethylhexanoic acid (1.32 mL, 8.25 mmol), and triethylamine (0.575 mL, 4.12 mmol) at 45 °C for 14 h. Ethyl acetate (15 mL) was then added and the mixture was extracted with water (containing 0.1% of trifluoroacetic acid). The aqueous phase was purified by preparative reverse phase HPLC (see Table 1) to give haptin **17a**, a lyophilized colorless powder. Mp: 175–180 °C (68 mg, 73%). ^1H -NMR (500 MHz, D_2O): 7.86, 7.70 (2d, 2 × 2H, $J = 8.5$); 4.89 (br s, 1H); 4.73 (s, 2H); 4.59 (s, 2H); 3.86 (m, 4H); 3.65 (m, 4H); 2.70 (m, 2H); 2.53 (m, 2H); 2.36 (m, 2H); 1.79 (m, 2H); 1.01 (t, 3H, $J = 7.5$). ^{13}C -NMR (125 MHz, D_2O): 178.3, 171.7, 167.8, 138.4, 135.7, 131.1, 130.0, 73.5, 68.8, 58.1, 56.5, 48.3, 38.0, 35.8, 27.4, 18.4, 13.8. HRMS: $\text{C}_{21}\text{H}_{30}\text{N}_3\text{O}_6\text{S}^+$ (M^+) calcd 452.1855, found 452.1860. IR (KBr): 3418, 3000, 2985, 1670, 1541, 1507, 1362, 1196.

A similar procedure starting with **16b** (0.100 g, 0.159 mmol) gave haptin **17b**, a colorless lyophilized powder. Mp: 201–203 °C (recryst from water) (88 mg, 94%). ^1H -NMR (500 MHz, D_2O): 7.86, 7.70 (2d, 2 × 2H, $J = 8$); 7.68 (s, 1H); 4.89 (br s, 1H); 4.73 (s, 2H); 4.60 (s, 2H); 3.86 (m, 4H); 3.66 (q, 4H, $J = 7$); 2.68 (t, 2H, $J = 7$); 2.53 (m, 2H); 2.36 (m, 2H); 1.76 (quint, 2H, $J = 7$); 1.30 (quint, 2H, $J = 7$); 0.85 (t, 3H, $J = 7$). ^{13}C -NMR (125 MHz, D_2O): 167.8, 135.6, 129.9, 73.5, 66.8, 56.4, 48.3, 38.1, 36.0, 31.1, 27.3, 23.9, 23.2, 14.8. HRMS: $\text{C}_{23}\text{H}_{33}\text{N}_3\text{O}_6\text{S}^+$ (M^+) calcd 480.2168, found 480.2172. IR (KBr): 3410, 2960, 1686, 1544, 1356, 1194.

1,4-Diaza-6-[(hexyloxy)imino]-4-hexylbicyclo[3.2.2]nonan-3-one (19). A suspension of **1** (0.453 g, 2.68 mmol) in acetonitrile (15 mL) was gently heated with *N*-(*tert*-butyldimethylsilyl)-*N*-trifluoroacetamide (3.2 mL, 13.7 mmol) until complete dissolution. After an additional 15 min at 25 °C, removal of the solvent and excess silylating agent in vacuo and purification by chromatography ($\text{CH}_2\text{Cl}_2/\text{MeOH}$ 30:1, $R_f = 0.28$) gave the silylated oxime (0.74 g, 98%). A solution of this silylated oxime (0.202 g, 0.714 mmol) in anhydrous DMF (2.5 mL) was treated with NaH (60% in mineral oil, 75 mg, 1.88 mmol) for 10 min at 20 °C. 1-Iodohexane (0.158 mL, 1.07

(32) The author has deposited atomic coordinates for this structure (**17b**) with the Cambridge Crystallographic Data Centre. The coordinates can be obtained, on request, from the Director, Cambridge Crystallographic Data Centre, 12 Union Road, Cambridge, CB2 1EZ, UK.

mmol) was added. After 3 h at 20 °C, the reaction was quenched with acetic acid (0.2 mL). Aqueous workup (CH₂Cl₂/water) and chromatography (CH₂Cl₂/MeOH 10:1, *R_f* = 0.53) gave **19** as colorless solid. Mp: 48–49 °C (0.163 g, 68%). ¹H-NMR (500 MHz, CDCl₃): 4.01 (t, 2H, *J* = 7); 3.91 (dd, 1H, *J* = 6, 1.6); 3.77 (d, 1H, *J* = 18); 3.74 (s, 2H); 3.71 (d, 1H, *J* = 18); 3.49 (ddd, 1H, *J* = 13.5, 9, 6); 3.39 (ddd, 1H, *J* = 13.5, 8.5, 6.5); 3.02 (m, 1H); 2.96 (m, 1H); 2.37 (m, 1H); 2.20 (m, 1H); 1.61 (m, 2H); 1.55 (m, 2H); 1.35–1.25 (m, 12H); 0.86 (m, 6H). ¹³C-NMR (125 MHz, CDCl₃): 171.8, 157.0, 74.4, 62.4, 54.1, 50.3, 48.9, 45.9, 31.6, 30.9, 29.0, 27.7, 26.4, 25.5, 22.5, 14.0. HRMS: C₁₉H₃₅N₃O₂ (M + Cs⁺) calcd 470.1784, found 470.1789. IR (CCl₄): 2957, 2931, 2854, 1646, 1467, 1138.

1-((4'-((2-((Allyloxy)carbonyl)ethyl)carbonyl)phenyl)methyl)-4-aza-3-oxo-6-(hydroxylimino)-4-hexylbicyclo[3.2.2]nonan-1-azonium Trifluoroacetate (20). A solution of **23** (28 mg, 0.082 mmol) and iodide **15** (162 mg, 0.43 mmol) in dry DMF (0.5 mL) was gently heated at 40–45 °C for 16 h. Acetonitrile (10 mL) and water (containing 0.1% TFA, 30 mL) were added. The precipitate was filtered off and washed with 5 × 40 mL of water/acetonitrile 3:1. Purification of the filtrate by preparative reverse-phase HPLC (see Table 1) gave **20** (30.5 mg, 61%). ¹H-NMR (300 MHz, CD₃OD): 8.72 (t, 1H, *J* = 7); 7.97, 7.70 (2d, 2 × 2H, *J* = 8); 5.93 (tdd, 1H, *J* = 17, 10.5, 5.8); 5.30 (dq, 1H, *J* = 17, 1.4); 5.20 (dq, 1H, *J* = 10.5, 1.4); 4.82 (s, 2H); 4.88, 4.72 (2d, 2 × 1H, *J* = 16); 4.60 (dt, 2H, *J* = 6, 1.4); 4.42 (s, 2H); 4.20 (dd, 1H, *J* = 5.4, 2.2); 4.13 (t, 2H, *J* = 7); 4.02, 3.86 (2m, 2 × 1H); 3.66 (m, 2H); 2.70 (t, 2H, *J* = 7); 2.55 (m, 2H); 1.66 (m, 2H); 1.42–1.21 (m, 6H); 0.90 (t, 3H, *J* = 7). MS (electrospray): (M⁺) 499.

1-((4'-((2-Carbonyl)ethyl)carbonyl)phenyl)methyl)-4-aza-3-oxo-6-(hydroxylimino)-4-hexylbicyclo[3.2.2]nonan-1-azonium Trifluoroacetate (2). A solution of **20** (30.5 mg, 0.050 mmol), triphenylphosphine (88 mg, 0.33 mmol), tetrakis(triphenylphosphine)palladium(0) (58 mg, 0.050 mmol), 2-ethylhexanoic acid (0.40 mL, 2.5 mmol), and triethylamine (0.17 mL, 1.24 mmol) in ethyl acetate (1.5 mL) was stirred at 45–50 °C for 2.5 h, diluted with ethyl acetate (25 mL), and extracted with dilute aqueous NaCl (containing 0.1% TFA, 6 × 25 mL). The combined aqueous phase was purified by preparative reverse-phase HPLC (see Table 1) to yield **2**, a colorless lyophilized powder. Mp: 113–115 °C (21 mg, 74%). ¹H-NMR (500 MHz, CD₃OD): 7.97, 7.71 (2d, 2 × 2H, *J* = 8.5); 4.82 (s, 2H); 4.86, 4.74 (2d, 2 × 1H, *J* = 18); 4.45, 4.41 (2d, 2 × 1H, *J* = 17); 4.19 (dd, 1H, *J* = 5, 2); 4.13 (t, 2H, *J* = 7); 3.98, 3.86 (2m, 2 × 1H); 3.64 (t, 2H, *J* = 7); 2.63 (t, 2H, *J* = 7); 2.59, 2.53 (2m, 2 × 1H); 1.68 (quint, 2H, *J* = 7); 1.40–1.25 (m, 6H); 0.91 (t, 3H, *J* = 7). ¹³C-NMR (125 MHz, CD₃OD): 168.8, 165.5, 148.0, 138.3, 134.8, 130.6, 129.4, 76.6, 72.9, 66.3, 58.4, 57.3, 46.0, 37.3, 34.8, 32.8, 30.0, 28.2, 26.5, 23.6, 14.4. HRMS: C₂₄H₃₅N₄O₅ (M⁺) calcd 459.2607, found 459.2613. IR (CH₃CN): 3628, 2939, 1692, 1180, 1126.

1,4-Diaza-6-[(tert-butyl)dimethylsilyl]oximino]-4-(propylsulfonyl)bicyclo[3.2.2]nonan-3-one (22). The silylated derivative of oxime **1** (0.222 g, 0.783 mmol) was dissolved in 20 mL of THF and treated with NaH (60% in mineral oil, 0.115 g, 2.88 mmol). After 30 min. at 25 °C, 1-propanesulfonyl chloride (0.86 mL, 7.6 mmol) was slowly added. The reaction was stirred for 3 h at 25 °C and then refluxed for 1 h. Quenching with acetic acid (0.2 mL), solvent removal in vacuo, and chromatography (hexane/ethyl acetate 3:2, TLC 1:1, 2 isomers in 4 to 1 ratio, *R_f* = 0.40 and 0.28) gave **22** (0.29 g, 95%). The pure major isomer (*R_f* = 0.40), a colorless solid, was characterized. Mp: 96–97 °C. ¹H-NMR (500 MHz, CDCl₃): 5.17 (dd, 1H, *J* = 5, 2); 3.87 (dd, 1H, *J* = 19, 1); 3.84 (dd, 1H, *J* = 19, 1); 3.69 (d, 1H, *J* = 19); 3.63 (dd, 1H, *J* = 19, 1); 3.57 (ddd, 1H, *J* = 14, 10.6, 5.3); 3.35 (ddd, 1H, *J* = 14, 10.5, 5.5); 3.07 (m, 2H); 2.45–2.37 (m, 1H); 2.22–2.15 (m, 1H); 1.81–1.75 (m, 1H); 1.73–1.65 (m, 1H); 0.98 (t, 3H, *J* = 7.5); 0.87 (s, 9H); 0.11, 0.09 (2s, 2 × 3H). ¹³C-NMR (125 MHz, CDCl₃): 174.6, 160.1, 63.3, 56.0, 50.9, 49.6, 45.3, 30.0, 25.7, 17.8, 16.7, 12.5. HRMS: C₁₆H₃₁N₃O₄SSi (M + Cs⁺) calcd 522.6859, found 522.6865. IR (CCl₄): 2931, 2858, 1690, 1462, 1364, 1160. Anal. Calcd: C, 49.33; H, 8.02; N, 11.08; S, 8.23. Found C, 49.34; H, 8.28; N, 11.02; S, 7.97.

1-((2-((4'-((Allyloxy)carbonyl)ethyl)carbonyl)phenyl)methyl)-4-aza-3-oxo-6-(hydroxylimino)-4-(propylsulfonyl)bicyclo[3.2.2]nonan-1-azonium Trifluoroacetate (23). A solution of the sultam **22** (0.301 g, 0.772 mmol) and iodide **15** (0.183 g, 0.491 mmol) in *N,N*-dimethylformamide (1 mL) was gently heated to 45 °C. Three additional portions of 0.14 g of iodide **15** were added after 1.5, 4, and 7 h. After a total reaction time of 14 h at 45 °C, the reaction was diluted with acetonitrile (10 mL) and water (containing 0.1% TFA, 40 mL), thoroughly shaken, and kept at 25 °C for 3 h. The precipitate was filtered off and washed with water (5 × 40 mL containing 0.1% CF₃COOH), and the filtrate purified by preparative reverse phase HPLC (see Table 1) to give **23**, a lyophilized colorless powder. Mp: 114–116 °C (0.40 g, 82%). ¹H-NMR (300 MHz, D₂O): 7.68, 7.55 (2d, 2 × 2H, *J* = 8); 5.74 (ddt, 1H, *J* = 17, 10.5, 5); 5.27 (dd, 1H, *J* = 5, 1); 5.13 (dd, 1H, *J* = 17); 5.04 (br d, 1H, *J* = 10.5); 4.72 (s, 2H); 4.55 (m, 4H); 4.43 (d, 2H, *J* = 5); 3.88 (m, 1H); 3.72 (m, 1H); 3.56–3.45 (m, 4H); 2.62–2.46 (m, 4H); 1.58 (quint, 2H, *J* = 7.5); 0.82 (t, 3H, *J* = 7.5). HRMS: C₂₄H₃₃N₄O₄S⁺ (M⁺) calcd 521.2070, found 521.2076. IR (CH₃CN): 3368, 1736, 1694, 1538, 1200, 1166, 1127.

1-((4'-((2-Carbonyl)ethyl)carbonyl)phenyl)methyl)-4-aza-3-oxo-6-(hydroxylimino)-4-(propylsulfonyl)bicyclo[3.2.2]nonan-1-azonium Trifluoroacetate (3). A solution of **23** (48.4 mg, 76.3 μmol) in ethyl acetate/methylene chloride 1:1 (12 mL) was treated with triphenylphosphine (170 mg, 0.65 mmol), tetrakis(triphenylphosphine)palladium(0) (96 mg, 0.082 mmol), 2-ethylhexanoic acid (0.63 mL, 3.9 mmol), and triethylamine (0.27 mL, 2.0 mmol) at 35 °C for 3 h. Ethyl acetate (15 mL) was then added and the mixture was extracted with water (containing 0.1% of trifluoroacetic acid). The aqueous phase was purified by preparative reverse phase HPLC (see Table 1) to give haptin **3**, a colorless lyophilized powder. Mp: 136–138 °C (33.5 mg, 74%). ¹H-NMR (500 MHz, D₂O): 7.81, 7.69 (2d, 2 × 2H, *J* = 8.5); 5.37 (dd, 1H, *J* = 6.5, 2); 4.86, 4.82 (2d, 2 × 1H, *J* = 13); 4.79 (dd, 1H, *J* = 18, 2.4); 4.72–4.66 (m, 2H); 4.60 (dd, 1H, *J* = 18, 2.4); 3.99, 3.86 (2m, 2 × 1H); 3.59 (t, 2H, *J* = 7); 3.56 (m, 2H); 2.73–2.56 (m, 2H); 2.64 (t, 2H, *J* = 7.5); 1.68 (hex, 2H, *J* = 7.5); 0.93 (t, 3H, *J* = 7.5). ¹³C-NMR (125 MHz, D₂O): 178.1, 171.6, 166.1, 147.6, 138.5, 135.8, 130.1, 74.0, 67.1, 58.3, 58.0, 57.4, 50.2, 37.8, 35.4, 27.7, 18.3, 13.7. HRMS: C₂₅H₃₂N₅O₉S⁺ (M⁺) calcd 481.1751, found 481.1788. IR (KBr): 3422, 1685, 1654, 1364, 1200, 1163, 1128.

1-(((Propylsulfonyl)carbonyl)methyl)-1-((4'-((2-carbonyl)ethyl)carbonyl)phenyl)methyl)-3-(hydroxylimino)cyclohex-4-en-1-azonium Trifluoroacetate (24). A solution of sultam **23** (5.4 mg, 0.0085 mmol) in CH₂Cl₂ (1 mL) and ethyl acetate (0.5 mL) was heated at 40 °C for 3 h with tetrakis(triphenylphosphine) palladium(0) (13 mg, 0.0011 mmol), triphenylphosphine (18.5 mg, 0.07 mmol), and potassium 2-ethylhexanoate (71 mg, 0.39 mmol). The reaction was diluted with water (40 mL, containing 0.1% TFA) and washed with CH₂Cl₂ (5 mL). Preparative reverse-phase HPLC (see Table 1) of the aqueous solution yielded compound **24** (2.4 mg, 47%) as the only product. ¹H-NMR (300 MHz, D₂O): 7.64, 7.42 (2d, 2 × 2H, *J* = 8); 6.43 (d, 1H, *J* = 10.5); 6.10 (dt, 1H, *J* = 10.5, 1.5); 4.88, 4.82 (2d, 2 × 1H, *J* = 16); 4.71, 4.42 (2d, 2 × 1H, *J* = 16); 4.26 (br s, 2H); 3.80, 3.72 (2d, 2 × 1H, *J* = 16); 3.48 (t, 2H, *J* = 6); 3.10 (t, 2H, *J* = 8); 2.53 (t, 2H, *J* = 6.5); 1.58 (hex, 2H, *J* = 7.5); 0.86 (t, 3H, *J* = 7.5). MS (FAB⁺) (M⁺) 481.

Preparation of the NHS-Esters and Coupling to Carrier Proteins. A solution of haptin **17a** (20 mg, 0.035 mmol) in 0.5 mL of DMF was treated with *N*-hydroxysuccinimide (0.02 mL of a 3.65 M solution in DMF, 0.073 mmol) and 1-(3-(dimethylamino)propyl)-3-ethylcarbodiimide hydrochloride (0.04 mL of a 1.8 M solution in water, 0.072 mmol) at 20 °C for 3 h, diluted with 15 mL water and rapidly purified by preparative reverse-phase HPLC (see Table 1) to give **18a** as a colorless lyophilized powder (19 mg, 81%). Similar procedures gave **18b** (19 mg, 76%) from haptin **17b** (21 mg, 0.035 mmol), **21** (6.3 mg, 95%) from **2** (5.7 mg, 0.010 mmol), and **25** (1.8 mg, 7%) from **3** (22 mg, 0.037 mmol). These activated esters were approximately 95% pure by HPLC, containing 5% starting acid

that formed during collection of the HPLC fractions. These were used directly for coupling to carrier proteins as follows: Ester **18a** (19 mg, 0.029 mmol) was dissolved in 0.2 mL of water/DMF 1:1. A 0.05 mL portion was added to a solution of KLH (keyhole limpet hemocyanin, 9.7 mg) in 1.95 mL of PBS (10 mM phosphate, 160 mM NaCl in water, pH 7.4) and 0.15 mL was added to a solution of BSA (bovine serum albumin, 30 mg) in 2.85 mL of PBS. These solutions were kept at 4 °C for 24 h and then used directly for immunological work. Ester **18b** (18.5 mg, 0.027 mmol) was similarly combined with KLH (9.5 mg) and BSA (30 mg). Ester **21** (6.3 mg, 0.01 mmol) was dissolved in 0.5 mL of PBS containing 0.08 mL of DMF. A 0.21 mL portion of this solution was added to KLH (9.2 mg in 1.82 mL PBS), and 0.37 mL was added to BSA (16 mg in 3.16 mL PBS) and kept at 4 °C for 24 h. Ester **25** (1.6 mg, 0.0023 mmol) was dissolved in 0.017 mL of water/DMF 1:1 and combined with KLH (3.2 mg in 0.32 mL PBS) at 4 °C. After 1.5 h, the coupling reaction was complete as judged by HPLC, and the sample was frozen to -80 °C. The BSA conjugate was

prepared directly from the hapten. Thus acid **3** (10 mg, 0.017 mmol) in 0.1 mL of DMF was treated with *N*-hydroxysuccinimide (0.036 mmol) and EDC (0.036 mmol) for 2.5 h at 20 °C, and combined directly with BSA (11 mg in 0.87 mL PBS) at 4 °C for 2 h. This conjugate was purified by gel filtration over a PD-10 column (Sephadex G-25) eluting with PBS.

Acknowledgment. This work was supported in part by the Humboldt Stiftung, Germany (J.S.) and by the US National Institutes of Health (GM 49736 to J.-L.R.).

Supporting Information Available: ¹H-NMR spectra of compounds **2**, **3**, **6**, **9**, **10**, **16a**, **16b**, **17a**, **17b**, **19**, **20**, **23**, **24** (13 pages). This material is contained in libraries on microfiche, immediately follows this article in the microfilm version of the journal, and can be ordered from the ACS; see any current masthead page for ordering information.

JO962179V